

DOI: 10.1002/cmdc.201000326

# Thalidomide Derivatives for the Treatment of Neuroinflammation

Christiane Contino-Pépin,<sup>\*,[a]</sup> Audrey Parat,<sup>[a]</sup> Cindy Patinote,<sup>[a]</sup> Wendi A. Roscoe,<sup>[b]</sup> Stephen J. Karlik,<sup>[b]</sup> and Bernard Pucci<sup>\*,[a]</sup>

The precise mechanism-of-action of thalidomide remains uncertain and might differ between diseases and under different clinical condition. With implications in the treatment of a variety of inflammatory and autoimmune diseases, as well as for use as an anticancer agent, alone or in combination with established therapeutics, it is clear that thalidomide and its derivatives deserve further scrutiny. In particular, thalidomide was shown to be effective in a mouse model of multiple sclerosis

(MS), an autoimmune inflammatory disorder, called experimental autoimmune encephalomyelitis (EAE). Herein, we describe the synthesis and preliminary biological evaluation of new macromolecular prodrugs of thalidomide bearing an aminoalkyl group on the phthalimide ring. The effectiveness of these compounds to limit EAE was investigated, and it was shown that, at 100 mg kg<sup>-1</sup> thalidomide-equivalent dose, they abrogated the clinical and pathological features of EAE.

## Introduction

Thalidomide first became known worldwide because of its tragic teratogenic effects. Subsequently, it was re-evaluated for use in the treatment of erythema leprosum nodosum (ENL).<sup>[1]</sup> Recently, thalidomide has been investigated for its promising therapeutic potential in various disorders.<sup>[2–4]</sup> Today, thalidomide is being evaluated for the treatment of a variety of inflammatory and autoimmune diseases,<sup>[5,6]</sup> and numerous hematological and solid or nonsolid malignancies.<sup>[7,8]</sup> More than twenty clinical trials include thalidomide in their regimen, alone or in combination with other antineoplastic drugs.<sup>[9]</sup> In 2006, thalidomide and its structural analogue lenalidomide (CC-5013, Revlimid) were approved by the Food and Drug Administration (FDA, USA) for combination treatment with dexamethasone for relapsed or refractory multiple myeloma.<sup>[10,11]</sup>

The precise mechanism-of-action of thalidomide remains uncertain and might differ between diseases and under different clinical condition.<sup>[12]</sup> Among the numerous modes-of-action ascribed to thalidomide, it has been postulated that the effect of the drug involves modulation of several cytokines associated with neovascular growth, such as vascular endothelial growth factor (VEGF), basic fibroblast growth factor (bFGF), hepatocyte growth factor (HGF), as well as tumor necrosis factor- $\alpha$  (TNF- $\alpha$ ) and several interleukins.<sup>[4,5,13]</sup> Recent studies have proposed that the anti-inflammatory and antiangiogenic effects of thalidomide might be due to a blockade of nuclear factor-kappa B (NF- $\kappa$ B) activation,<sup>[14]</sup> or an inhibitory effect on cyclooxygenase enzymes (COX-1/2).<sup>[15,16]</sup> Thalidomide was able to restore blood-brain barrier (BBB) permeability and provide neuroprotection in amyloid  $\beta_{1-42}$  or quinolinic acid-injected brain models.<sup>[17,18]</sup> In addition, D'Amato et al.<sup>[19]</sup> demonstrated significant antiangiogenic activity of thalidomide on corneal angiogenesis induced by VEGF.

Angiogenesis, defined as the development of new blood vessels from pre-existing vasculature, is a natural process that

occurs in both normal physiology and disease.<sup>[20]</sup> Although this phenomenon is a critical event for the maintenance, proliferation and metastasis of tumors,<sup>[21–23]</sup> angiogenesis has been implicated in the evolution of autoimmune inflammatory disorders, such as rheumatoid arthritis and multiple sclerosis (MS). Karlik and co-workers reported altered spinal cord vascularization in the C57L6 mouse model for MS called experimental autoimmune encephalomyelitis (EAE).<sup>[24,25]</sup>

We have been engaged in the development and synthesis of thalidomide analogues as potential therapeutic tools. For angiogenesis inhibition, we designed macromolecular amphipathic carriers endowed with multiple thalidomide units. These compounds exhibited a significant ability to inhibit angiogenesis in a mouse model of corneal neovascularization when compared to thalidomide.<sup>[26]</sup> We recently described a novel class of thalidomide analogues substituted on the phthalimide ring system. Among the several structural modifications on the phthalimide ring, the introduction of either a carboxylic function or an *N*-(aminopropyl)amino group at the C4 position led to a reduction of clinical signs of EAE.<sup>[27]</sup> These results suggested that angiogenesis could be an interesting target for interfering with inflammatory MS-like pathophysiology. In the present report, our strategy was to enhance the activity of *N*-(ami-

[a] Dr. C. Contino-Pépin, Dr. A. Parat, C. Patinote, Prof. B. Pucci  
Laboratoire de Chimie Bioorganique et des Systèmes Moléculaires Vectoriels, Faculté des sciences, Université d'Avignon et des Pays de Vaucluse  
33 rue Louis Pasteur, 84000 Avignon (France)  
Fax: (+33) 49014-4449  
E-mail: christine.pépin@univ-avignon.fr  
bernard.pucci@univ-avignon.fr

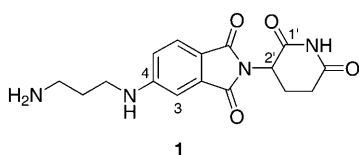
[b] Dr. W. A. Roscoe, Prof. S. J. Karlik  
University of Western Ontario, Department of Medical Imaging, LHSC-UC  
339 Windermere Road, London, Ontario, N6A 5A5 (Canada)

Supporting information for this article is available on the WWW under <http://dx.doi.org/10.1002/cmdc.201000326>.

nopropyl)-4-amino thalidomide by appending oligomeric multivalent carriers, called telomers.

For many years, we have studied the biomedical potential of low-weight polymers derived from tris(hydroxymethyl)amino-methane (Tris).<sup>[28]</sup> These compounds are obtained by free-radical polymerization of an acryloyl monomer derived from tris(hydroxymethyl)acrylamidomethane (THAM) in the presence of an alkane or a perfluoroalkane thiol as a transfer reagent called telogen. The physicochemical parameters of these telomers (molecular weight, hydrophilic–lipophilic balance, electric charge) can be adjusted through both the starting material and the experimental conditions.<sup>[29,30]</sup> With regard to their biological properties, we previously showed that these multifunctional carriers are able to cross physiological membranes and diffuse through all tissue types.<sup>[31]</sup> A whole-body autoradiography performed on rat and mouse allowed us to confirm the ubiquitous biodistribution of THAM-derived telomers in all biological compartments except the brain.<sup>[32]</sup> Moreover, after intravenous (iv) or oral (po) administration to rat, these compounds were slowly released within 100 h, and no toxicity was observed. Finally, the anchorage of various antitumor agents, such as cytosine arabinoside (Ara-C) or 5-fluorouracil (5-Fu), to the polymeric backbone gave macromolecular prodrugs with improved bioavailability and a better therapeutic index than the parent drugs.<sup>[28,33]</sup>

Herein, we describe the synthesis of a series of telomers with *N*-(aminopropyl)-4-amino thalidomide **1** appended. The synthesis of **1** was recently reported and is shown in

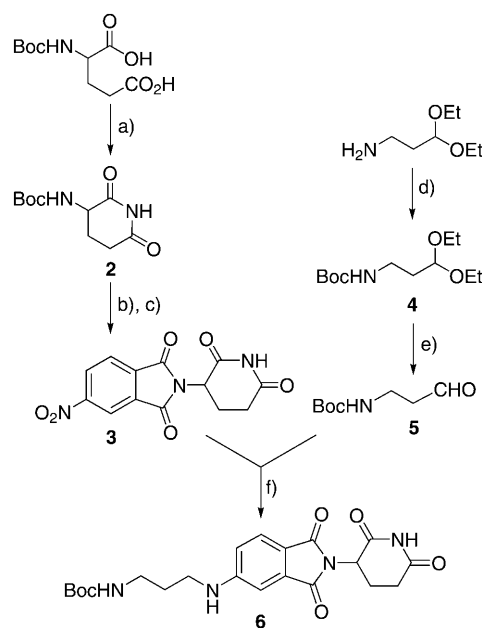


Scheme 1.<sup>[27]</sup> According to the hydrophobic nature of thalidomide, and to the structure–activity relationships gained from previous biological experiments, this thalidomide derivative was conjugated to variable cotelomers of Tris end-capped with a hydrophilic tail.

## Results and Discussion

### Chemistry

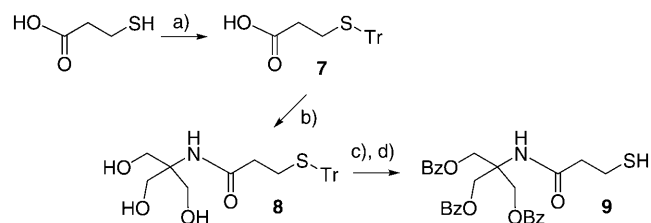
Synthesis of thalidomide analogue **6** was performed as previously reported (Scheme 1). Briefly, the preparation of nitro derivative **3** started by cyclization of *N*-*tert*-butyloxycarbonyl-L-glutamic acid in the presence of trifluoroacetamide following the method of Galons et al.<sup>[34]</sup> Subsequent deprotection of the resulting *N*-Boc glutarimide **2** with trifluoroacetic acid (TFA) gave the corresponding TFA salt. Subsequent condensation of this intermediate with 4-nitrophthalic anhydride by refluxing overnight in glacial acetic acid<sup>[35]</sup> led to 4-nitro-substituted thalidomide **3** in 70% yield. Finally, the reductive amination of **3** in the presence of **5**, previously obtained in two steps from 1-



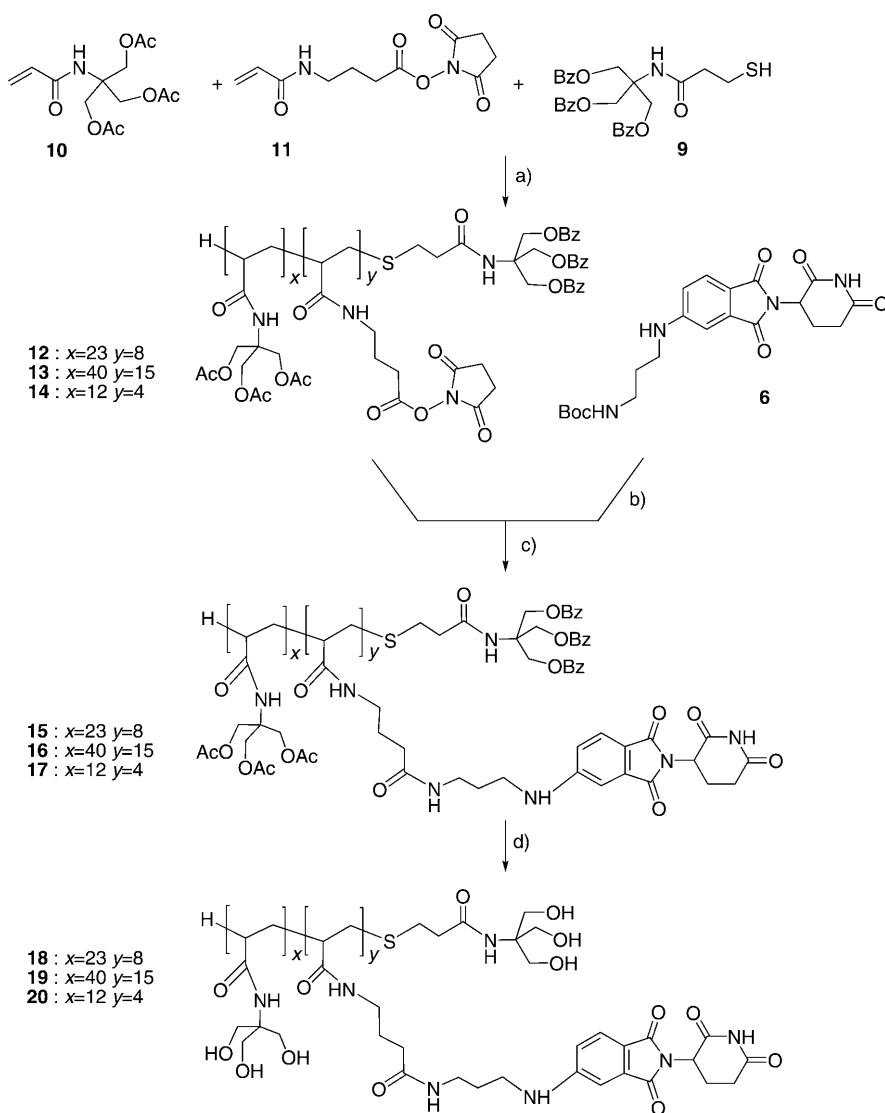
**Scheme 1.** Reagents and conditions: a)  $\text{CF}_3\text{CONH}_2$ ,  $\text{Et}_3\text{N}$ , HOBT, EDC-Cl,  $\text{CH}_2\text{Cl}_2$ ,  $0^\circ\text{C} \rightarrow \text{RT}$ , 24 h, 95%; b)  $\text{CF}_3\text{CO}_2\text{H}/\text{CH}_2\text{Cl}_2$  (7:3),  $0^\circ\text{C} \rightarrow \text{RT}$ , 1 h, 100%; c) 4-nitrophthalic anhydride, AcOH, molecular sieves (4 Å), reflux, 48 h, 70%; d)  $(\text{Boc})_2\text{O}$ ,  $\text{Et}_3\text{N}$ , dioxane,  $0^\circ\text{C} \rightarrow \text{RT}$ , o/n, 90%; e) AcOH,  $\text{H}_2\text{O}$ , RT, 4 h, 98%; f)  $\text{H}_2$ , Pd/C, DMF/THF (9:1), RT, 16 h, 70%. EDC, 1-ethyl-3-(3-dimethylamino-propyl)carbodiimide; HOBT, hydroxybenzotriazole.

amino-3,3-diethoxypropane,<sup>[36]</sup> provided compound **6** in satisfactory yield. Notably, compound **6** is a yellow fluorophore; after removal of the *N*-Boc protecting groups, its maximum excitation and emission in water are 276 nm and 552 nm, respectively (data not shown). Thalidomide **6** was used as the starting material for the subsequent attachment of each telomer.

Telogen *N*-((trisbenzyloxymethyl)-methyl)-3-mercapto-propionamide **9**, was synthesized in four consecutive steps from 3-mercaptopropionic acid (Scheme 2).<sup>[37]</sup> Co-telomerization reactions (Scheme 3) between tris(acetoxymethyl)acrylamidomethane monomer **10** and  $\gamma$ -amino propionic acid-derived acrylamide monomer **11**,<sup>[31]</sup> in the presence of telogen **9** as a transfer reagent and azobisisobutyronitrile (AIBN) as a radical initiator, were carried out under an inert atmosphere in refluxing THF. Telomerization was continued until complete consumption of starting monomers (monitored by TLC). Telomers **12–14**



**Scheme 2.** Reagents and conditions: a) triphenylmethyl chloride (1.1 equiv),  $\text{CH}_2\text{Cl}_2$ , RT, 16 h, 94%; b) Tris (1.1 equiv), EEDQ (1.2 equiv), EtOH, reflux, 12 h, 85%; c)  $\text{C}_6\text{H}_5\text{COCl}$  (4.5 equiv),  $\text{Et}_3\text{N}$  (9 equiv),  $\text{CH}_2\text{Cl}_2$ , RT, 12 h, 82%; d) TFA/ $\text{CH}_2\text{Cl}_2$  (2:8),  $0^\circ\text{C} \rightarrow \text{RT}$ , o/n, 100%. EEDQ, 2-ethoxy-1-ethoxycarbonyl-1,2-dihydroquinoline; TFA, trifluoroacetic acid; Tris, tris(hydroxymethyl)aminomethane.



**Scheme 3.** Reagents and conditions: a) AIBN, THF,  $N_2$ , reflux, 16 h, 56% for **12**, 70% for **13** and 55% for **14**; b) TFA,  $CH_2Cl_2$  (5:5),  $0^\circ C \rightarrow RT$ , 1 h, 100%; c)  $Et_3N$ , THF, RT,  $N_2$  atmosphere, 4 days, 80% for **15**, 83% for **16** and 99% for **17**; d) MeONa (cat.), MeOH, RT, o/n, 100%. AIBN, azobisisobutyronitrile; TFA, trifluoroacetic acid.

were prepared by using different ratio of monomers **10** and **11**, and purified by size-exclusion chromatography. The degree of polymerization (DPn) is defined as the average number of repeating units in the polymeric backbone plus one (the telogen moiety). The DPn depends on the ratio of telogen/monomers, adjusted through both starting materials and experimental conditions.<sup>[29]</sup> The DPn value was determined by proton NMR in combination with UV analysis.

Previously, we demonstrated that Tris-derived polymers cannot be characterized using gel permeation chromatography (GPC) measurements.<sup>[37]</sup> A study performed by matrix-assisted laser desorption/ionization time-of-flight mass spectrometry (MALDI-TOF-MS) also yielded inconsistent results (not published), probably due to the variable fragmentation behavior of the telomers during the MALDI experiments. This disparity between results observed for synthetic polymers has already

been reported in the literature and ascribed to both instrument and sample preparation parameters used for the MALDI-MS analysis.<sup>[38]</sup> In such conditions, these two techniques were ruled out for telomer characterization.

The use of compound **9** as a telogen agent in this synthetic route is relevant for two reasons: 1) to allow facile NMR estimation of the DPn by comparing the total area of typical signals for each monomer to well-identified aromatic signals ascribed to the telogen part; and 2) to support the NMR estimation by UV calibration, since in this case polymeric units do not interfere with UV absorbance of telogen end-caps on the polymer backbone.

$^1H$  NMR analysis permitted the determination of  $x$  and  $y$  values (Scheme 3) by comparing the area of the peaks assigned to six *ortho*-aromatic protons in the telogen moiety (doublet;  $\delta = 8$  ppm, integral 6H) to the signal ascribed to methylene protons of monomer **10** (singlet;  $\delta = 4.4$  ppm, integral 6 $\cdot$  $x$ -H) and to succinimidyl protons of **11** (singlet;  $\delta = 2.9$  ppm, integral 4 $\cdot$  $y$ -H). These  $^1H$  NMR data were supported by UV measurements (see Supporting Information).

NMR determinations, although suitable for short telomers, become inaccurate as the size of telomers increases. For this reason, we used the UV absorbance

of benzoyl groups from the telogen moiety in combination with the NMR data for more precise DPn estimation. The three benzoyl groups appended on the Tris moiety of the telogen agent strongly absorb at  $\lambda = 230$  nm. A calibration curve of the absorbance versus the molar concentration of telogen **9** was first established using standard solutions (0–70  $\mu M$ ) in a 1:1 mixture of dichloromethane and methanol. Triplicate samples of telomer were analyzed; in each case, a precise weight of telomers **12–14** was dissolved in the solvent system, defining the weight concentration of telomer **12–14** in  $g L^{-1}$  ([telomer]<sup>W</sup>). This solution was diluted to a concentration suitable for UV measurements. The value of the UV absorbance provided the molar concentration of the telogen **9** ( $mol L^{-1}$ ) in solution ([telogen]<sup>M</sup>). The average molecular weight of the cotelomer ( $\langle MW \rangle$ ) was then calculated using Equation (1), with errors within  $\pm 3\%$ :

$$\langle MW \rangle_{\text{telomer}} = [\text{telomer}]^W / [\text{telogen}]^M \quad (1)$$

Since each co-telomer backbone contains a single telogen moiety, the average molecular mass of the co-telomer can be derived. The DPn of the co-telomer was determined by combining  $^1\text{H}$  NMR and UV data through Equation (2):

$$\langle MW \rangle_{\text{telomer}} = MW_{\text{TA}} + [(x \cdot MW_{\text{Tris}}) + (y \cdot MW_{\text{AA}})] \quad (2)$$

where  $MW_{\text{TA}}$  is the molecular mass of the telogen agent **9**,  $MW_{\text{Tris}}$  and  $MW_{\text{AA}}$  those of monomers **10** and **11**, respectively, and  $x+y$  is the total number of monomers in the backbone. The average degree of polymerization (DPn) is then easily obtained from Equation (3):

$$\text{DPn} = (x+y)+1 \quad (3)$$

At the same concentration used for the UV calibration ( $\sim 0.5 \text{ g L}^{-1}$ ), no absorbance was observed at  $\lambda = 230 \text{ nm}$  for a co-telomer devoid of phenyl groups. No degradation of the benzoyl groups was observed by proton NMR when the pure telogen agent was reacted with AIBN in refluxing THF. Therefore, the ester bonds of the telogen agent are stable during telomerization. We combined the  $x/y$  ratio from the proton NMR data with this to determine the DPn of the telomers. At low DPn, the molecular weights obtained by proton NMR alone were found to be in good agreement with that obtained by the combination of NMR and UV data.

Subsequent removal of the protecting group of thalidomide amino derivative **6** with TFA and condensation to telomers **12–14** produced telomers **15–17**. Final treatment under Zemplén conditions yielded the desired telomers **18–20** in satisfactory yields; NMR analysis confirmed the total disappearance of aromatic groups of telogen.

### Multiple sclerosis animal model

To induce experimental autoimmune encephalomyelitis (EAE), C57L6 mice were immunized with MOG<sub>35–55</sub> peptide. Each immunization contained a mixture of MOG peptide in complete Freund's adjuvant (CFA) supplemented with *Mycobacterium tuberculosis*. Mice were given intraperitoneal (ip) injections of *Bordetella pertussis* toxin on the day of immunization, and on day two post-immunization.

The clinical signs of EAE include a limp tail, and affected or paralyzed limbs. The clinical scoring scale was: 0.0: healthy; 1: limp tail; 1.5: poor righting reflex but tail is no longer limp (recovery only); 2.0: poor righting reflex with limp tail; 3.0: above signs as well as one hind limb affected; 3.5: above signs as well as one hind limb paralyzed; 4.0: above signs as well as both hind limbs affected; 4.5: above signs as well as both hind limbs paralyzed; 5.0: moribund. On the first day of clinical signs (clinical score = 1), the mice were treated with compounds **18** or **19** ( $100 \text{ mg kg}^{-1}$  or  $1 \text{ mg kg}^{-1}$  thalidomide-equivalent dose) via ip injections, and treatments were continued daily for seven days. Compound **20**, with a low number of thalidomide pendants, was not tested in these preliminary experi-

ments. Control mice were also treated on the first day they showed clinical signs with daily ip injections of sterile phosphate-buffered saline (PBS). The mice were sacrificed on the eighth day, and the spinal cord was dissected, fixed in 10% neutral-buffered formalin, embedded in paraffin wax, and sectioned into  $5 \mu\text{m}$  sections. Histological slides were prepared using hematoxylin–eosin and solochrome cyanine R. Slides were scored blindly according to a published pathological scoring scale.<sup>[25]</sup> Differences between clinical and pathological scores were determined by a Mann–Whitney U test for non-parametric data, with  $p < 0.05$  considered to be significant.

In parallel to this study, the effect of free thalidomide on EAE mice was investigated at two different doses ( $100$  and  $200 \text{ mg kg}^{-1}$  po). Since free thalidomide was effective at inhibiting angiogenesis and inflammation in other studies, it was used here as a positive control.<sup>[39,40]</sup> Treatment also began on the first day of clinical signs of the disease. Mice were also treated for seven days and sacrificed on the eighth day. Spinal cords were dissected and processed as described above.

Mice immunized with MOG<sub>35–55</sub> to induce EAE began showing clinical signs 10–15 days post-immunization. They were randomized into PBS control or treatment groups once they showed clinical signs of illness and were then treated for seven days. The mean clinical scores for compounds **18** and **19** are illustrated in Figure 1a ( $1 \text{ mg kg}^{-1}$ ) and Figure 1b ( $100 \text{ mg kg}^{-1}$ ). The mean clinical scores for free thalidomide given orally at  $100 \text{ mg kg}^{-1}$  or  $200 \text{ mg kg}^{-1}$  are shown in Figure 2a. Pathological evaluations for both experiments are shown in Figure 1c and Figure 2b.

At enrolment, all mice were at a clinical score of at least 1. During the experimental period, the vehicle controls showed an increase in clinical signs of disease, which decreased partially by the end of the observation period. Compound **18** yielded decreased disease even when given at a thalidomide-equivalent dose of  $1 \text{ mg kg}^{-1}$  ( $p < 0.05$ ). The disease was very mild at  $100 \text{ mg kg}^{-1}$  thalidomide-equivalent dose of compounds **18** and **19** ( $p < 0.001$  for **18**;  $p < 0.026$  for **19**), and some mice achieved a score of 0, or complete reversal of all clinical signs. Figure 1c shows the scores for the blinded pathological assessments. The mean scores for inflammation and demyelination for all treatments were somewhat lower than the saline controls and reached statistical significance for compound **19** when dosed at  $100 \text{ mg kg}^{-1}$ . The combination of decreased clinical score and pathological score for compound **19** is consistent with anti-inflammatory activity. As a consequence, the decrease in demyelination score is an indication that myelin damage was decreased, resulting from reduced inflammation compared to controls.

In a previous experiment,  $100 \text{ mg kg}^{-1}$  of free thalidomide was ineffective in this model when administered by ip injection.<sup>[27]</sup> Although thalidomide administered orally was effective in decreasing clinical and pathological signs of EAE, it was not as effective as compounds **18** and **19**. Therefore, we have achieved disease reversal with these new compounds at lower doses.

However, on the basis of the ability of telomers to reach the bloodstream after oral administration,<sup>[32]</sup> and considering that

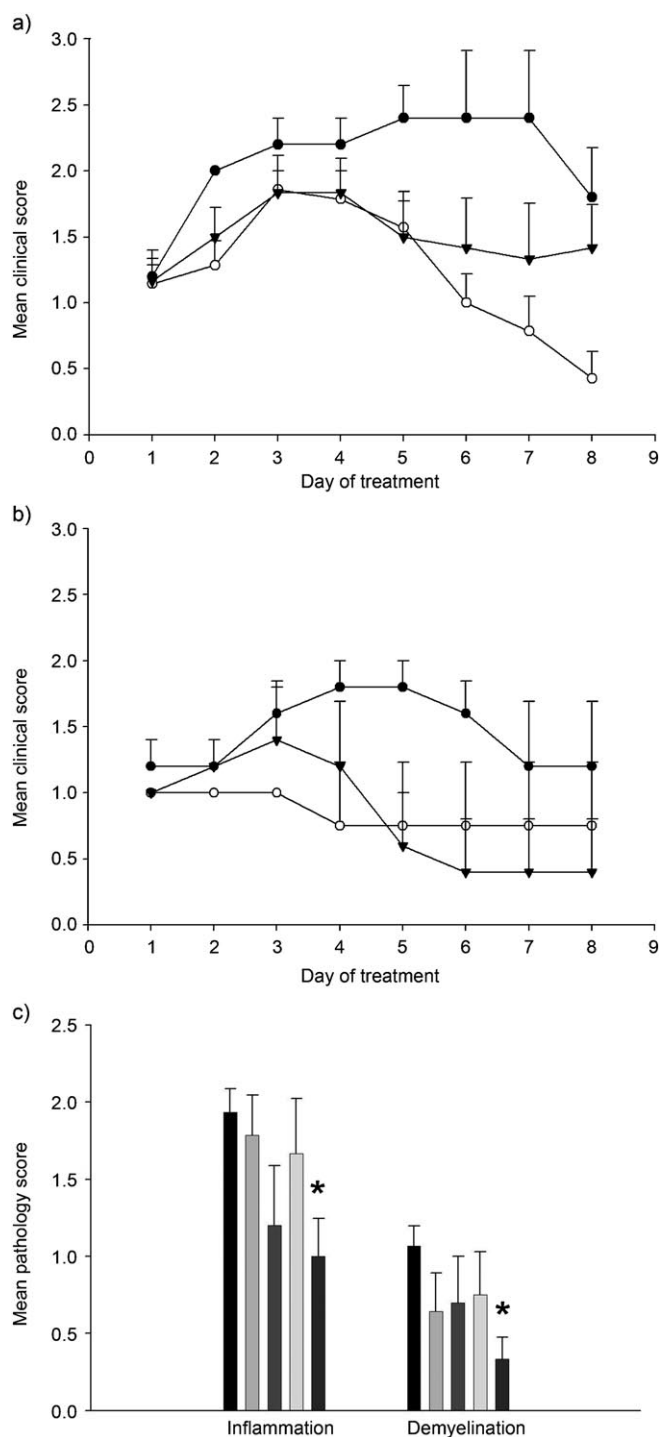


**Figure 1.** a) and b) Mean clinical scores and b) pathological scores for EAE mice treated with vehicle (●), or compounds **18** (○) and **19** (▼) at 1 mg kg<sup>-1</sup> (panel a) and 100 mg kg<sup>-1</sup> (panel b); (\*  $p < 0.05$ ). Error bars indicate the standard error of the mean.

free thalidomide is more active when given orally, further investigation of *N*-(aminopropyl)amino-thalidomide telomers is necessary to specify both the best dose and mode of administration in the EAE mouse model of MS.

Two factors could account for increased activity with compounds **18** and **19** after ip injection: enhanced general bio-

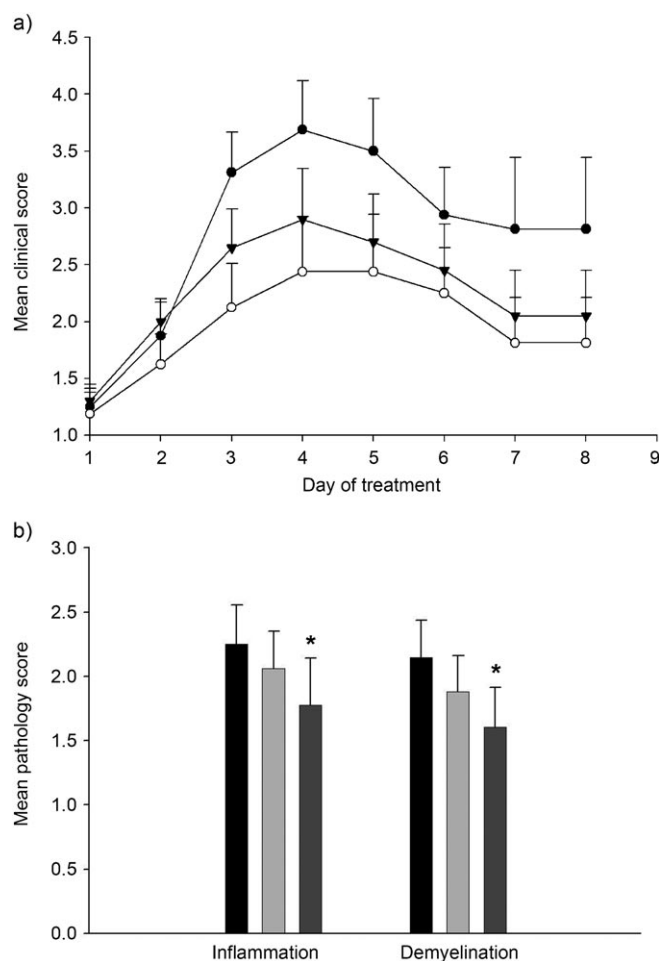


**Figure 2.** a) Mean clinical scores and b) pathological scores for EAE mice treated orally with vehicle (●; ■), or free thalidomide (100 mg kg<sup>-1</sup>: ○; ■; 200 mg kg<sup>-1</sup>: ▼; ■). Mice treated with 100 mg kg<sup>-1</sup> of free thalidomide showed fewer clinical signs of EAE. Mice treated with 200 mg kg<sup>-1</sup> of free thalidomide showed fewer pathological signs of EAE (\*  $p < 0.05$ ). Error bars indicate the standard error of the mean.

availability due to structural modification of the parent thalidomide, and/or multiple appending of the active component on the same carrier. Considering the hydrophobic character of thalidomide, conjugation to a hydrophilic moiety might be expected to enhance activity. Thus, *N*-(aminopropyl)-4-amino thalidomide appears to be a promising thalidomide derivative when appended to a hydrophilic macromolecular carrier, compared to the parent drug. In addition to a possible synergistic effect gained from multiplicity, the efficacy against EAE might arise through enhanced permeability and retention at sites of BBB impairment.<sup>[41]</sup>

*N*-(aminopropyl)amino-thalidomide telomers **18** and **19** achieved substantial success in the reversal of clinical signs of acute EAE in mice. All animals exhibited definite clinical signs on entry into the study, so this was a treatment study and not a prevention study. Our findings can be compared to recent results obtained by McLarnon et al., who demonstrated thalidomide-mediated neuroprotection and reduced vascular remodeling in an excitotoxin-injected brain model.<sup>[18]</sup> We expect a similar effect with the use of telomers endowed with *N*-(ami-

nopropyl)amino-thalidomide in the EAE model, particularly as VEGF-induced vascular changes have been observed by inhibition experiments using SU5416 (Semaxinib).<sup>[25]</sup> To ascertain whether the mechanism of action is that of antiangiogenesis, further investigation is required, in particular to identify the molecular targets of these agents. The optical properties of these new fluorescent derivatives will permit future histological assays.

## Conclusions

The aim of this work was to synthesize and evaluate thalidomide analogues as agents against neuroinflammation. Previously, we demonstrated the therapeutic potency of thalidomide derivatives in angiogenesis inhibition<sup>[26]</sup> and EAE.<sup>[27]</sup> Although we cannot yet provide details on the precise mechanism of action of thalidomide and its derivatives, herein we have shown enhanced activity from molecular modifications of thalidomide and proposed new therapeutic applications for this "re-discovered" old drug.

## Experimental Section

### Chemistry

Reactions and the homogeneity of the compounds were monitored by thin layer chromatography (TLC; Merck F<sub>254</sub> silica plates) visualized under UV light ( $\lambda = 254$  and  $366$  nm) or by spraying with a 5% H<sub>2</sub>SO<sub>4</sub> solution in EtOH, and/or a 5% ninhydrin solution in EtOH followed by heating at  $\sim 150^\circ\text{C}$  to detect characteristic groups. Flash chromatography was carried out on Merck silica gel Gerduran Si 60 (40–63  $\mu\text{m}$ ). Size-exclusion chromatography was carried out using Sephadex LH-20 resin or Sephadex G-25 resin (GE Healthcare Bio-Sciences AB). Final products were purified by high-pressure liquid chromatography (HPLC) on a Varian Pro Star Microsorb C<sub>18</sub> column (5  $\mu\text{m}$  granulometry,  $4.6 \times 250$  mm or  $21.4 \times 250$  mm). Melting points were determined in open capillary tubes and are uncorrected. <sup>1</sup>H, <sup>13</sup>C and DEPT NMR spectra were recorded on a Bruker AC-250 spectrometer (<sup>1</sup>H, 250 MHz; <sup>13</sup>C, 62.86 MHz). Chemical shifts ( $\delta$ ) are given in ppm relative to the solvent residual peak as a heteronuclear reference. Abbreviations used for signal patterns are: s (singlet), d (doublet), t (triplet), q (quartet), m (multiplet). UV-Vis spectra were recorded on a Cary Win Varian spectrophotometer with a double-compartment quartz (Suprasil) cell (length = 10 mm). High resolution mass spectrometry (HRMS) was recorded on a QStar Elite (Applied Biosystems SCIEX) spectrometer equipped with an atmospheric pressure ionization (API) source (ESI+, ToF). HRMS data was collected by the Spectropole, Faculté des Sciences et Techniques de Saint-Jérôme (Marseille, France).

**2'-N-(tert-Butyloxycarbonyl)aminoglutaramide (2):** Trifluoroacetamide (2.7 g, 24.2 mmol) was added to a solution of *N*-tert-(butyloxycarbonyl)glutamic acid (5 g, 20.2 mmol), HOBt (6 g, 44.0 mmol), and Et<sub>3</sub>N (8.5 mL, 60.5 mmol) in CH<sub>2</sub>Cl<sub>2</sub> (50 mL) at 0 °C. EDCI (8.14 g, 42.5 mmol) was added, and the mixture was allowed to reach RT. After consumption of glutamic acid (24 h), water (30 mL) was added. The organic layer was washed with saturated aq Na<sub>2</sub>CO<sub>3</sub> (2 × 100 mL) and brine (2 × 100 mL), and dried (Na<sub>2</sub>SO<sub>4</sub>), filtered and concentrated in vacuo. Crystallization (EtOAc) gave **2** as a white powder (4.4 g, 95%), no further purification was necessary for the next step: *R*<sub>f</sub> = 0.67 (EtOAc); mp: 193.7–194.4 °C; [ $\alpha$ ]<sub>D</sub><sup>20</sup> = –63 (*c* = 1, DMF); <sup>1</sup>H NMR (250 MHz, [D<sub>6</sub>]DMSO):  $\delta$  = 10.70 (s, 1 H), 7.14

(d, *J* = 8.65 Hz, 1 H), 4.22 (m, 1 H), 2.69 (m, 1 H), 2.47 (m, 2 H), 1.92 (m, 1 H), 1.39 ppm (s, 9 H); <sup>13</sup>C NMR (63 MHz, [D<sub>6</sub>]DMSO):  $\delta$  = 24.5, 28.2, 31.0, 50.4, 78.2, 172.5, 173.0 ppm.

**2'-(4-Nitrophthaloyl)glutaramide (3):** Compound **2** (1.7 g, 7.4 mmol) was treated with a mixture of TFA and CH<sub>2</sub>Cl<sub>2</sub> (7:3; 10 mL) and stirred at RT for 1 h. The corresponding TFA salt precipitated from the reaction mixture, and excess TFA was removed in vacuo (quantitative yield). The TFA salt (1.8 g) was added to a solution of 4-nitrophthalic anhydride (1.62 g, 8.41 mmol) and molecular sieves (4 Å) in acetic acid (25 mL). The mixture was heated at reflux for 2 d, and then filtered through Celite and washed with EtOAc. The organic solvents were removed in vacuo, and the crude compound was purified by flash chromatography (cyclohexane/EtOAc; 20 → 0%). Recrystallization from EtOAc/*n*-hexane gave **3** as a white powder (1.57 g, 70%): *R*<sub>f</sub> = 0.49 (EtOAc/cyclohexane; 6:4); mp: 226.8–227.8 °C; [ $\alpha$ ]<sub>D</sub><sup>20</sup> = +1.47 (*c* = 1, DMF); <sup>1</sup>H NMR (250 MHz, [D<sub>6</sub>]DMSO):  $\delta$  = 11.20 (s, 1 H), 8.68 (d, *J* = 8.1 Hz, 1 H), 8.57 (s, 1 H), 8.20 (d, *J* = 8.1 Hz, 1 H), 5.24 (dd, *J* = 5.2, 12.7 Hz, 1 H), 2.89 (m, 1 H), 2.50 (m, 2 H), 2.13 ppm (m, 1 H); <sup>13</sup>C NMR (63 MHz, [D<sub>6</sub>]DMSO):  $\delta$  = 22.3, 31.3, 49.9, 118.9, 125.5, 130.6, 133.0, 136.2, 152.2, 165.7, 166.0, 173.2 ppm; HRMS-ESI+: *m/z* [*M*+H]<sup>+</sup> calcd for C<sub>13</sub>H<sub>9</sub>N<sub>3</sub>O<sub>6</sub>: 304.0564, found: 304.0565.

**2'-(4-(N-(N-tert-Butyloxycarbonyl)propylamino)phthaloyl)glutaramide (6):** 3-*N*-(tert-butyloxycarbonyl)aminopropanal (0.342 g, 1.98 mmol), obtained from 1-amino-3,3-diethoxypropane following the method of Bi et al.,<sup>[34]</sup> was dissolved in anhydrous THF/DMF (9:1; 10 mL). 2'-(4-Nitrophthaloyl)glutaramide (0.5 g, 1.65 mmol) and catalytic Pd/C (10% in weight) were then added to the solution. The mixture was stirred at RT under H<sub>2</sub> (8 bars) for 16 h. After consumption of the starting material, the reaction was filtered through Celite and concentrated in vacuo. Purification by flash chromatography (EtOAc/cyclohexane; 3:7) gave **6** as a yellow powder (0.71 g, 70%): *R*<sub>f</sub> = 0.71 (EtOAc/cyclohexane; 8:2); mp: 89.3 °C; [ $\alpha$ ]<sub>D</sub><sup>20</sup> = +5.7 (*c* = 1, CH<sub>2</sub>Cl<sub>2</sub>); <sup>1</sup>H NMR (250 MHz, CDCl<sub>3</sub>):  $\delta$  = 8.14 (s, 1 H), 7.61 (d, *J* = 8.3 Hz, 1 H), 7.02 (s, 1 H), 6.79 (d, *J* = 8.7 Hz, 1 H), 5.49 (m, 1 H), 4.95 (dd, *J* = 4.8, 11.8 Hz, 1 H), 4.71 (m, 2 H), 3.23–3.33 (m, 4 H), 2.78–2.98 (m, 3 H), 2.21 (m, 1 H), 1.79 (qt, *J* = 6.2 Hz, 2 H), 1.48 ppm (s, 9 H); <sup>13</sup>C NMR (63 MHz, CDCl<sub>3</sub>):  $\delta$  = 22.8, 28.4, 29.1, 37.5, 40.1, 49.0, 79.8, 105.9, 116.6, 117.8, 125.5, 134.6, 153.7, 156.6, 167.5, 168.0, 168.9, 171.4 ppm; HRMS-ESI+: *m/z* [*M*+H]<sup>+</sup> calcd for C<sub>21</sub>H<sub>26</sub>N<sub>4</sub>O<sub>6</sub>: 431.1925, found: 431.1925.

**Co-telomers bearing peracetylated Tris and succinimidyl moieties (12–14):** Monomers **10** and **11** (see Table 1 for ratios) were dissolved in anhydrous THF under N<sub>2</sub>. Appropriate amounts of telogen **9** and radical initiator AIBN were added, and the mixture was stirred at reflux under N<sub>2</sub> until complete consumption of monomers ( $\sim 12$ –24 h). The mixture was concentrated in vacuo and purified by size-exclusion chromatography (CH<sub>2</sub>Cl<sub>2</sub>/MeOH; 1:1) to give co-telomers **12–14** as white powders (56% for **12**, 70% for **13**, and 55% for **14**). Their DP<sub>n</sub> values (see Table 2) were calculated using <sup>1</sup>H NMR data and confirmed by UV measurements (see Supporting Information).

**Co-telomers bearing peracetylated Tris and N-(aminopropyl)-4-aminothalidomide moieties (15–17):** Co-telomer (**12–14**) was dissolved in anhydrous THF. Deprotected compound **6** (deprotected using TFA/CH<sub>2</sub>Cl<sub>2</sub> (3:7); see HRMS data in the Supporting Information) was added to the solution in excess (relative to active ester groups; 1.3 equiv per succinimidyl moiety). Et<sub>3</sub>N was used to adjust and maintain pH 8. The mixture was stirred at RT for 4 d under N<sub>2</sub> and protected from light. Concentration in vacuo and purification by size-exclusion chromatography (MeOH/CH<sub>2</sub>Cl<sub>2</sub>; 5:5)

**Table 1.** Initial conditions for the synthesis of co-telomers 12–14.

Co-telomer	Molar ratio (amount [mg])						AIBN
	9		10		11		
12	1	(100)	15	(865)	5	(243)	0.5 (15.7)
13	1	(200)	45	(5190)	15	(1460)	0.5 (31.4)
14	1	(100)	15	(865)	5	(243)	0.5 (15.7)

**Table 2.** Experimental data for co-telomers 12–14.

Co-telomer	Structure <sup>[a]</sup>		DPn <sup>[b]</sup>	Yield [%]	Mw [g mol <sup>-1</sup> ]
	x	y			
12	23	8	32	56	9476
13	40	15	56	70	16371
14	12	4	17	55	5149

[a] Average number of peracetylated Tris (x) and thalidomide derivative (y) monomer units. [b] DPn: degree of polymerization. The number of monomer units (x and y) in the polymer backbone + 1 (DPn = x + y + 1).

gave co-telomers 15–17 as yellow powders (80% for 15, 83% for 16, and 99% for 17). At this point, the coupling ratio of *N*-(aminopropyl)-4-aminothalidomide was specified as described in the main body of the manuscript. Notably, for each telomer, NMR structural evaluation showed that the proportion of thalidomide moieties was similar to the succinimidyl groups in the precursor telomers 12–14 (see Table 3).

**Table 3.** Experimental data for co-telomers 15–17.

Co-telomer	Structure <sup>[a]</sup>		DPn <sup>[b]</sup>	Yield [%]	Mw [g mol <sup>-1</sup> ]
	x	y			
15	23	8	32	80	11196
16	40	15	56	83	19596
17	12	4	17	99	6009

[a] Average number of peracetylated Tris (x) and thalidomide derivative (y) monomer units. [b] DPn: degree of polymerization. The number of monomer units (x and y) in the polymer backbone + 1 (DPn = x + y + 1).

**Co-telomers bearing Tris and *N*-(aminopropyl)-4-aminothalidomide moieties (18–20):** Co-telomer (15–17) was dissolved in MeOH under N<sub>2</sub> and treated with catalytic NaOMe (0.5 mol% per telomer). After stirring at RT for 12 h, IRC-50 resin was added to neutralize the solution. The mixture was shaken for 15 min, filtered and concentrated in vacuo, and purified by size-exclusion chromatography on a Sephadex G-25 gel (H<sub>2</sub>O). The appropriate fractions were lyophilized to give co-telomers 18–20 as yellow powders (quantitative yield).

### Multiple Sclerosis Animal Model

Six-week-old female C57L6 mice (Jackson Laboratories, Bar Harbor, ME) were immunized by subcutaneous injection in the hind flank with 200 µg of MOG<sub>35–55</sub> peptide (Sheldon Biochemical; Montreal, Canada). Each immunization contained a 1 mg mL<sup>-1</sup> mixture of 100 mg of MOG peptide in CFA (Difco Laboratories; Michigan, USA) supplemented with 400 ng of *M. tuberculosis* (Difco Laboratories; Michigan, USA). Mice were given 200 ng ip injections of *B. per-*

*tussis* toxin (List Biological Laboratories, Cedarlane; Hornby, Canada) on the day of immunization and on day two post-immunization. Mice were housed in a light- and temperature-controlled environment, with a 12 h day/night cycle at 21–23 °C, and received food and water ad libitum.

On the first day of clinical symptoms, mice were treated with compounds 18 and 19 at 100 or 1 mg kg<sup>-1</sup> thalidomide-equivalent dose (100 mg kg<sup>-1</sup>: 18, n = 7; 19, n = 6; 1 mg kg<sup>-1</sup>: 18, n = 6; 19, n = 6). Treatments were carried out daily for seven days. Control mice (n = 5 and n = 4 for the two dose groups) were also treated on the first day they showed clinical signs with daily ip injections of 0.1 mL sterile PBS. The mice were sacrificed on the eighth day, their spinal cord was dissected, fixed in 10% neutral-buffered formalin, embedded in paraffin wax, and sectioned into 5 µm sections. Histological slides were prepared using hematoxylin-eosin and solochrome R cyanin. Slides were scored blindly according to a published pathological scoring scale.<sup>[25]</sup>

As a positive control, free thalidomide was administered to EAE mice at 100 (n = 8) and 200 mg Kg<sup>-1</sup> (n = 9); a control using vehicle was also conducted (n = 8). Treatment began on the first day of clinical signs of disease. Mice were treated for seven days and sacrificed on the eighth day. Spinal cords were dissected and processed as described above.

All animals used in this study were maintained and handled in accordance with the International Guiding Principles for Biomedical Research Involving Animals and using protocols approved by the Animal Use Subcommittee of the University of Western Ontario (Canada).

**Keywords:** angiogenesis · multiple sclerosis · neuroinflammation · telomers · thalidomide

- [1] S. K. Teo, K. E. Resztak, M. A. Scheffler, K. A. Kook, J. B. Zeldis, D. I. Stirling, S. D. Thomas, *Microbes Infect.* **2002**, *4*, 1193–1202.
- [2] J. J. Wu, D. B. Huang, K. R. Pang, S. Hsu, S. K. Tying, *Br. J. Dermatol.* **2005**, *153*, 254–273.
- [3] S. M. Capitosti, T. P. Hansen, M. L. Brown, *Bioorg. Med. Chem.* **2004**, *12*, 327–336.
- [4] L. Rosiñol, M. T. Cibeira, M. Segarra, M. C. Cid, X. Filella, M. Aymerich, M. Rozman, L. Arenillas, J. Esteve, J. Bladé, E. Montserrat, *Cytokine* **2004**, *26*, 145–148.
- [5] A. Thiele, R. Bang, M. Gütschow, M. Rossol, S. Loos, K. Eger, G. Tiegs, S. Hauschildt, *Eur. J. Pharmacol.* **2002**, *453*, 325–334.
- [6] H. W. Man, L. G. Corral, D. I. Stirling, G. W. Muller, *Bioorg. Med. Chem. Lett.* **2003**, *13*, 3415–3417.
- [7] P. Musto, *Leukemia* **2004**, *18*, 325–332.
- [8] S. R. Porter, J. Jorge Jr., *Oral Oncol.* **2002**, *38*, 527–531.
- [9] S. Sleijfer, W. H. J. Kruit, G. Stoter, *Eur. J. Cancer* **2004**, *40*, 2377–2382.
- [10] M. Melchert, A. List, *Int. J. Biochem. Cell Biol.* **2007**, *39*, 1489–1499.
- [11] C. Hulin, *La revue de médecine interne* **2007**, *28*, 682–688.
- [12] T. D. Stephens, C. J. W. Brunde, B. J. Fillmore, *Biochem. Pharmacol.* **2000**, *59*, 1489–1499.
- [13] F. E. Kruse, A. M. Jousen, K. Rohrschneider, M. D. Becker, H. E. Völcker, *Graefes Arch. Clin. Exp. Ophthalmol.* **1998**, *236*, 461–466.
- [14] J. A. Keifer, D. C. Guttridge, B. P. Ashburner, A. S. Baldwin Jr., *J. Biol. Chem.* **2001**, *276*, 22382–22387.
- [15] T. Noguchi, R. Shimazawa, K. Nagasawa, Y. Hashimoto, *Bioorg. Med. Chem. Lett.* **2002**, *12*, 1043–1046.
- [16] G. J. Du, H. H. Lin, Q. T. Xu, M. W. Wang, *Aesculape Vascular Pharm.* **2005**, *43*, 112–119.
- [17] J. K. Ryu, J. G. McLarnon, *Neurobiol. Dis.* **2008**, *29*, 254–266.
- [18] J. K. Ryu, N. Jantarantotai, J. G. McLarnon, *Neuroscience* **2009**, *163*, 601–608.

- [19] R. J. D'Amato, M. S. Loughnan, E. Flynn, J. Folkman, *Proc. Natl. Acad. Sci. USA* **1994**, *91*, 4082–4085.
- [20] S. Liekens, E. De Clercq, J. Neyts, *Biochem. Pharmacol.* **2001**, *61*, 253–270.
- [21] J. Folkman, *New Engl. J. Med.* **1971**, *285*, 1182–1186.
- [22] F. A. Shepherd, S. S. Sridhar, *Lung Cancer* **2003**, *41* (Suppl. 1), 63–72.
- [23] J. Folkman, *J. Natl. Canc. Inst.* **1990**, *82*, 4–6.
- [24] S. Kirk, J. A. Frank, S. Karlik, *J. Neurol. Sci.* **2004**, *217*, 125–130.
- [25] W. A. Roscoe, M. E. Welsh, D. E. Carter, S. J. Karlik, *J. Neuroimmunol.* **2009**, *209*, 6–15.
- [26] S. Périno, C. Contino-Pépin, R. Satchi-Fainaro, C. Butterfield, B. Pucci, *Bioorg. Med. Chem. Lett.* **2004**, *14*, 421–425.
- [27] C. Contino-Pépin, A. Parat, S. Périno, C. Lenoir, M. Vidal, H. Galons, S. Karlik, B. Pucci, *Bioorg. Med. Chem. Lett.* **2009**, *19*, 878–881.
- [28] C. Contino-Pépin, J. C. Maurizis, B. Pucci, *Curr. Med. Chem.* **2002**, *9*, 645–665.
- [29] B. Pucci, E. Guy, F. Vial-Reveillon, A. A. Pavia, *Eur. Polym. J.* **1988**, *24*, 1077–1086.
- [30] B. Pucci, J. C. Maurizis, A. A. Pavia, *Eur. Polym. J.* **1991**, *27*, 1101–1106.
- [31] F. Chehade, J. C. Maurizis, B. Pucci, A. A. Pavia, M. Ollier, A. Veyre, F. Escaig, C. Jeanguillaume, R. Dennebouy, G. Slodzian, E. Hindie, *Cell. Mol. Biol.* **1996**, *42*, 335–342.
- [32] J. C. Maurizis, M. Azim, M. Rapp, B. Pucci, A. A. Pavia, J. C. Madelmont, A. Veyre, *Xenobiotica* **1994**, *24*, 535–541.
- [33] S. Jasseron, C. Contino-Pépin, J. C. Maurizis, M. Ollier, B. Pucci, *Eur. J. Med. Chem.* **2003**, *38*, 825–836.
- [34] N. Flaih, C. Pham-Huy, H. Galons, *Tetrahedron Lett.* **1999**, *40*, 3697–3698.
- [35] G. W. Muller, R. Chen, S. Y. Huang, L. G. Corral, L. M. Wong, R. T. Patterson, Y. Chen, G. Kaplan, D. I. Stirling, *Bioorg. Med. Chem. Lett.* **1999**, *9*, 1625–1630.
- [36] W. Bi, J. Cai, S. Liu, M. Baudy-Floc'h, L. Bi, *Bioorg. Med. Chem.* **2007**, *15*, 6909–6919.
- [37] K. S. Sharma, G. Durand, F. Giusti, B. Olivier, A. S. Fabiano, P. Bazzacco, T. Dahmane, C. Ebel, J. L. Popot, B. Pucci, *Langmuir* **2008**, *24*, 13581–13590.
- [38] S. J. Wetzel, C. M. Guttman, J. E. Girard, *Int. J. Mass Spectrom.* **2004**, *238*, 215–225.
- [39] T. Asano, H. Kume, F. Taki, S. Ito, Y. Hasegawa, *Biol. Pharm. Bull.* **2010**, *33*, 1028–1032.
- [40] T. A. Faivre-Chauvet, P. Thomare, G. Deleris, K. Estieu-Gionnet, A. Bikfalvi, J. Barbet, F. Paris, *J. Nucl. Med.* **2010**, *51*, 624–631.
- [41] A. V. Kabanov, H. E. Gendelman, *Prog. Polym. Sci.* **2007**, *32*, 1054–1082.

---

Received: August 3, 2010

Revised: September 13, 2010

Published online on October 8, 2010